and 4000 K along the magma ocean isentrope, Fig. 3). The Rayleigh number lies in the regime of turbulent convection: The presence of turbulence may substantially influence the settling of crystals as they form upon cooling. The surface heat flux, $F \sim 6 \times 10^4$ W m^{-2}, estimated from mixing length theory far exceeds the incoming solar flux (*30*) and suggests that the surface temperature was set by heat exchange of the magma ocean with a dense silicate atmosphere rather than by solar radiation balance (*2*). This value of F implies a cooling time for the magma ocean ~20 ky (*30*). In fact, a number of processes are likely to increase the cooling time of the magma ocean substantially, including crystallization, which is predicted to initiate in the mid-mantle (*28*) and to separate the magma ocean into upper and basal layers (*31*). The evolution at this stage also depends strongly on the viscosity, which will set the time scale for buoyancy-driven motion of crystals and liquid that can lead to chemical differentiation. The direction of motion will be set by the crystal-liquid density contrast, the sign of which varies with pressure and temperature. Indeed, crystals are expected to float near the base of the mantle (*16*), producing a buoyantly stable basal magma layer that may be long-lived (*31*).

References and Notes

1. R. M. Canup, *Icarus* **168**, 433 (2004).
2. V. S. Solomatov, in *Evolution of the Earth*, D. Stevenson, Ed., vol. 9 of *Treatise on Geophysics*, G. Schudbert, Ed. (Elsevier, Amsterdam, 2007), p. 91.
3. S. E. Haggerty, V. Sautter, *Science* **248**, 993 (1990).
4. J. Revenaugh, S. A. Sipkin, *Nature* **369**, 474 (1994).
5. Q. Williams, E. J. Garnero, *Science* **273**, 1528 (1996).
6. G. Urbain, Y. Bottinga, P. Richet, *Geochim. Cosmochim. Acta* **46**, 1061 (1982).
7. I. Kushiro, H. S. Yoder Jr., B. O. Mysen, *J. Geophys. Res.* **81**, 6351 (1976).
8. Y. Bottinga, P. Richet, *Geochim. Cosmochim. Acta* **59**, 2725 (1995).
9. J. E. Reid *et al.*, *Phys. Earth Planet. Inter.* **139**, 45 (2003).
10. H. Behrens, F. Schulze, *Am. Mineral.* **88**, 1351 (2003).
11. D. Tinker *et al.*, *Am. Mineral.* **89**, 1701 (2004).
12. C. Liebske *et al.*, *Earth Planet. Sci. Lett.* **240**, 589 (2005).
13. E. A. Wasserman, D. A. Yuen, J. R. Rustad, *Earth Planet. Sci. Lett.* **114**, 373 (1993).
14. D. J. Lacks, D. Rear, J. A. Van Orman, *Geochim. Cosmochim. Acta* **71**, 1312 (2007).
15. D. Nevins, F. J. Spera, M. S. Ghiorso, *Am. Mineral.* **94**, 975 (2009).
16. L. Stixrude, B. B. Karki, *Science* **310**, 297 (2005).
17. M. Mookherjee, L. Stixrude, B. B. Karki, *Nature* **452**, 983 (2008).
18. Computations were performed by using the VASP software (*32*) with the local density approximation and ultrasoft pseudopotentials as before (*16*, *17*, *26*). Methods are available as supporting material on *Science* Online.
19. L. A. Lange, *Rev. Mineral.* **30**, 331 (1994).
20. M. L. Rivers, I. S. E. Carmichael, *J. Geophys. Res.* **92**, (B9), 9247 (1987).
21. J. Mungall, *Geochim. Cosmochim. Acta* **66**, 125 (2002).
22. T. K. Wan, T. S. Duffy, S. Scandolo, R. Car, *J. Geophys. Res.* **112** (B3), 03208 (2007).
23. G. Giordano, D. B. Dingwell, *Earth Planet. Sci. Lett.* **208**, 337 (2003).
24. C. A. Angell, P. A. Cheeseman, S. Tamaddon, *Science* **218**, 885 (1982).
25. C. A. Angell, *Science* **267**, 1924 (1995).
26. B. B. Karki, D. Bhattarai, M. Mookherjee, L. Stixrude, *Phys. Chem. Miner.* **37**, 103 (2010).
27. E. M. Stolper, *Geochim. Cosmochim. Acta* **46**, 2609 (1982).
28. L. Stixrude, N. de Koker, N. Sun, M. Mookherjee, B. B. Karki, *Earth Planet. Sci. Lett.* **278**, 226 (2009).
29. The Rayleigh and Prandtl numbers are $Ra = [\alpha\rho g(T_M - T_S)L^3]/(\kappa\eta)$ and $Pr = \eta/(\rho\kappa)$. We have adopted the density (ρ = 4410 kg m^{-3}) and thermal expansivity ($\alpha = 2.6 \times 10^{-5}$) (*16*) and assumed the depth scale L = 3000 km, acceleration due to gravity g = 10 m s^{-2}, thermal conductivity k = 1.2 W m^{-1} K^{-1} (*33*), thermal diffusivity $\kappa = k/(\rho c_P)$ where the specific heat c_P = 1660 J kg^{-1} K^{-1} (*16*), a mantle potential temperature T_M = 2500 K, the lowest temperature at which the mantle will be completely molten, and a surface temperature T_S = 1000 K set by a dense atmosphere (*2*).
30. The surface heat flux is $F = 0.22k(T_M - T_S)Ra^{2/7}Pr^{-1/7}L^{-1}$ (*34*) and the cooling time is $\tau_{cool} = T_M c_P M_M / 4\pi R^2 F$, where M_M is the mass of the mantle and R is the radius of Earth.
31. S. Labrosse, J. W. Hernlund, N. Coltice, *Nature* **450**, 866 (2007).
32. G. Kresse, J. Furthmuller, *Comput. Mater. Sci.* **6**, 15 (1996).
33. A. M. Hofmeister, A. G. Whittington, M. Pertermann, *Contrib. Mineral. Petrol.* **158**, 381 (2009).
34. B. I. Shraiman, E. D. Siggia, *Phys. Rev. A* **42**, 3650 (1990).
35. K. R. Harris, L. A. Woolf, M. Kanakubo, *J. Chem. Eng. Data* **50**, 1777 (2005).

36. This work was supported by NSF (EAR-0809489) and the UK National Environmental Research Council (NE/F01787/1). Computing facilities were provided by the Center of Computation and Technology at Louisiana State University. The authors thank J. Brodholt, M. Ghiorso, and S. Karato for useful comments and suggestions.

Supporting Online Material

www.sciencemag.org/cgi/content/full/328/5979/740/DC1
Materials and Methods
Figs. S1 and S2

16 February 2010; accepted 7 April 2010
10.1126/science.1188327

Extreme Deuterium Excesses in Ultracarbonaceous Micrometeorites from Central Antarctic Snow

J. Duprat,[1]* E. Dobrică,[1] C. Engrand,[1] J. Aléon,[1] Y. Marrocchi,[2] S. Mostefaoui,[2] A. Meibom,[2] H. Leroux,[3] J.-N. Rouzaud,[4] M. Gounelle,[2] F. Robert[2]

Primitive interplanetary dust is expected to contain the earliest solar system components, including minerals and organic matter. We have recovered, from central Antarctic snow, ultracarbonaceous micrometeorites whose organic matter contains extreme deuterium (D) excesses (10 to 30 times terrestrial values), extending over hundreds of square micrometers. We identified crystalline minerals embedded in the micrometeorite organic matter, which suggests that this organic matter reservoir could have formed within the solar system itself rather than having direct interstellar heritage. The high D/H ratios, the high organic matter content, and the associated minerals favor an origin from the cold regions of the protoplanetary disk. The masses of the particles range from a few tenths of a microgram to a few micrograms, exceeding by more than an order of magnitude those of the dust fragments from comet 81P/Wild 2 returned by the Stardust mission.

The light element isotopic compositions of undifferentiated interplanetary material provide insights into the physicochemical processes that took place in the coldest regions of the early solar system. Large deuterium excesses are expected in the solid component(s) of comets because their water and HCN molecules exhibit D/H ratios from 2 to 15 times the terrestrial value, respectively (*1*). However, isotopic measurements of fragments of comet 81P/Wild 2 returned by the Stardust mission show moderate D/H ratios that do not exceed three times the terrestrial value, possibly indicating a substantial alteration during impact capture process (*2*). By contrast, large D/H ratios have been observed as micrometer-sized hot spots in organic matter of interplanetary dust particles (IDPs) (*3*, *4*) or primitive meteorites (*5*, *6*). These D excesses may have been inherited from the cold molecular cloud that predated the protosolar nebula (*3*, *5*, *7*) or may be the result of a local process that occurred in the cold outer regions of the protoplanetary disk (*8*, *9*). The nature of the D-rich hot spots and their relationship to the organic matter bulk composition remain a matter of debate (*6*, *10*). Organic matter in meteorites is sparse and disseminated in the matrix, with a maximum bulk concentration on the order of a few weight percent (wt %) (*11*). It is mainly accessible as the acid-insoluble component (IOM) remaining after demineralization of large amounts (grams) of primitive meteorites.

Large numbers of Antarctic micrometeorites (AMMs), which are IDPs with sizes ranging from 20 to 1000 μm, can be recovered from the Antarctic ice cap (*12*). Here, we describe AMMs obtained from the melting and sieving of 3 m^3 of ultraclean snow that fell in the vicinity of the French-Italian CONCORDIA station at Dome C

[1]Centre de Spectrométrie Nucléaire et de Spectrométrie de Masse, Université Paris-Sud 11, CNRS/IN2P3, F-91405 Orsay, France. [2]Laboratoire de Minéralogie et Cosmochimie du Muséum (LMCM), UMR 7202–CNRS INSU, Muséum National d'Histoire Naturelle, 57 Rue Cuvier, 75231 Paris Cedex 05, France. [3]Unité Matériaux et Transformations, Université Lille 1 & CNRS, 59655 Villeneuve d'Ascq, France. [4]Laboratoire de Géologie de l'Ecole Normale Supérieure, UMR CNRS 8538, 24 rue Lhomond, 75231 Paris Cedex 5, France.

*To whom correspondence should be addressed. E-mail: jean.duprat@csnsm.in2p3.fr

(75°S, 123°E) between 1955 and 1970 (i.e., before human activities started in the area) (*13*). Because they were recovered from snow rather than ice, they did not endure the mechanical stress or aqueous alteration that are typical of both meteorites and AMMs recovered from Antarctic ice (*14*). Within the unmelted AMM population exhibiting a fine-grained, fluffy texture with no evidence for substantial heating during atmospheric entry (i.e., vesicles and/or magnetite shell), we report mineralogical and isotopic studies of two particles (particles 19 and 119) characterized by exceptionally high carbon content (Fig. 1A), referred to as ultracarbonaceous Antarctic micrometeorites (UCAMMs) (*15*). Their carbonaceous component is present in the form of organic matter and represents 48% and 85% of the analyzed area of particles 19 and 119, respectively (*13*). The sizes of particles 19 and 119 before fragmentation were 80 μm by 50 μm and 275 μm by 110 μm, respectively.

High-resolution transmission electron microscopy (HRTEM) of the UCAMMs shows a poor structural organization of the organic matter, with nanometer-sized polyaromatic layers, single or stacked in groups of two or three (Fig. 1B). This fringe length has the same scale as that reported in HRTEM studies of IOMs from Murchison and Orgueil carbonaceous chondrites (*16*). Combined studies of field emission gun scanning electron microscopy (FEG-SEM) and analytical TEM reveal mineral assemblages embedded within the organic matter (Fig. 1C) consisting mainly of Mg-rich silicates and Fe-Ni sulfides. These fine-grained mineral assemblages contain both amorphous and crystalline phases (Fig. 1C). Some glassy aggregates are comparable to the glass with embedded metal and sulfides (GEMS) identified in IDPs (Fig. 2) (*13*). The crystalline fraction of particle 19 is dominated by fine-grained clumps of olivines, pyroxenes, and iron sulfides, with mineral sizes ranging from ~15 to ~500 nm and having a pronounced frequency peak around 100 nm.

Isotopic imaging on fragments of particles 19 and 119 reveals large D excesses associated with the carbon-rich areas (Fig. 3) (*13*). By contrast, the carbon ($^{12}C/^{13}C$) and oxygen ($^{18}O/^{16}O$) isotopic maps do not exhibit large isotopic anomalies (*13*). The highest D/H ratio of 4.6 (±0.5) × 10^{-3} [δD = 29,000 ± 3000 per mil (‰)] was measured within particle 119 (Fig. 3D). This ratio approaches that of the most D-rich hot spots observed by isotopic imaging in interplanetary material (*3*, *5*). However, the D enrichments in the UCAMMs we analyzed have occurred over much wider areas than those reported previously in extraterrestrial materials. The areas with D/H > 10^{-3} (δD > 5400‰) extend over 135 to 280 μm^2 and 65 to 200 μm^2 in particles 19 and 119, respectively (Fig. 3, A and C) (*13*). In the in situ isotopic imaging of IOM from primitive chondrites, the contribution of hot spots to the bulk D/H ratio remains small (*5*, *6*), whereas in the UCAMMs the areas with D/H ratios larger than 10 times the terrestrial value represent most of the analyzed surface (Fig. 4) (*13*). Because the average D/H ratio of the UCAMMs is compatible with that of D-rich hot spots reported in other interplanetary materials, it is conceivable that these hot spots may result from the fragmentation and/or alteration of a primitive organic matter component similar to that revealed by this study.

In the D/H versus C/H atomic ratio plot, the data from particles 19 and 119 cluster along a main trend going from a first component at C/H = 1 to 2 and D/H = 0.5 × 10^{-3} to 1 × 10^{-3} up to a high C/H component with C/H ratios ranging from 3 to 7 and D/H ratios ranging from 1 × 10^{-3} to 1.4 × 10^{-3} (Fig. 4) (*13*). The first component corresponds to that reported in bulk IOM analyses of CR carbonaceous chondrites (*10*). The nature of the UCAMM high C/H component remains to be clarified, but HRTEM data establish its highly disorganized structure and therefore rule out a substantial graphitization (Fig. 1B). The isotopic and elementary ratios of IOM from unequilibrated ordinary chondrites (UOCs) (*10*) plot along the same main trend

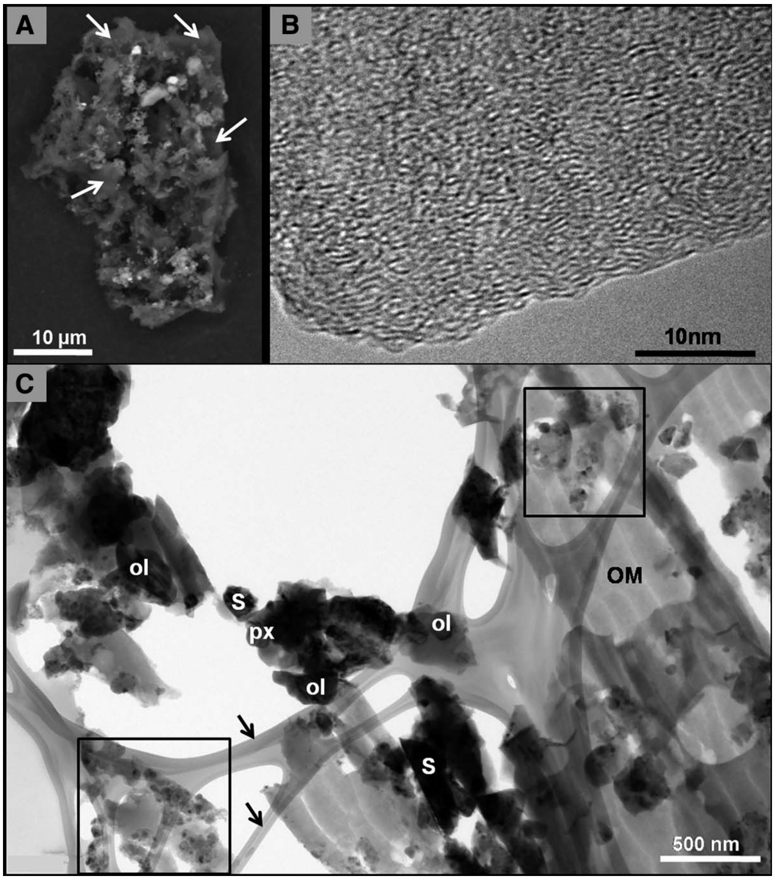

Fig. 1. (**A**) Backscattered scanning electron micrograph of particle 119. The carbon-rich areas appear dark (arrows); the bright inclusions are dominated by Fe-Ni sulfides and silicates. (**B**) High-resolution TEM image of particle 19. (**C**) Bright-field TEM image of particle 19. The lacey carbon film (*13*) is indicated as black arrows; the crystalline phases are Mg-rich olivines (ol), Mg-rich pyroxenes (px), and Fe-Ni sulfides (S); OM, organic matter. Glassy aggregates (GEMS candidates) are highlighted in black squares (*13*).

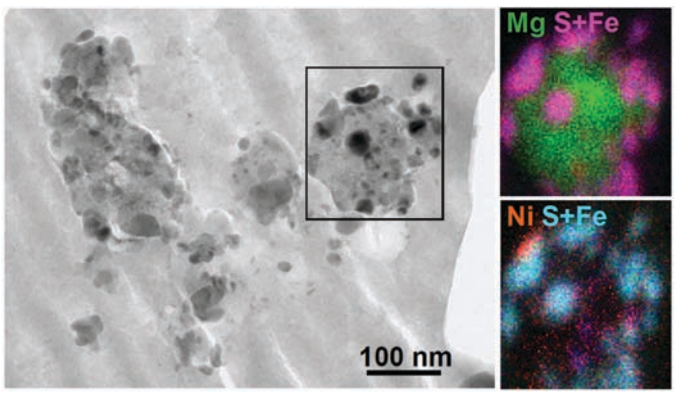

Fig. 2. (**Left**) Bright-field TEM image of a GEMS candidate embedded in the carbonaceous matter of particle 19. (**Right**) Stacked energy-dispersive x-ray spectroscopy elemental distribution maps of Mg, S + Fe (top) and Ni, S + Fe (bottom) for the GEMS candidate (black square).

(Fig. 4). It has been suggested that this main trend in UOCs may be due to a parent body process (*10*). However, it is difficult to conceive that the main trend from the UCAMMs may result from the same process, because (i) the UCAMMs and UOCs strongly differ both chemically and mineralogically [in particular, the UOC organic matter concentration (<0.5 wt %) (*10*) is much lower than that observed in UCAMMs]; (ii) we do not observe any sign of thermal processing of the UCAMMs and, by contrast to the UOCs, we observe for C/H > 3 a constant D/H plateau rather than a correlated increase of D/H with C/H (fig. S2) (*13*); and (iii) the data presented here (Fig. 3) show that the whole range of variation of the main trend coexists within a few tens of square micrometers, whereas the UOC main trend concerns IOM residues from the bulk meteorites. Therefore, the UCAMM main trend seems compatible with the sampling of a heterogeneous organic matter reservoir.

Above the main trend, the data broadly spread toward extreme D/H ratios with D/H > 2.5×10^{-3} and C/H = 2 to 6 (Fig. 4). The D-rich hot spots in IDPs for which C/H ratios have also been reported span a large range (0 < C/H < 3) (*4*), whereas the hot spots from IOMs of CR2 primitive chondrites have C/H ratios limited to a more restricted zone (1 < C/H < 1.5) (*5*). The UCAMM extreme D/H component seems to extend the high C/H trend observed in IDPs, including particles collected during the meteor shower associated with comet 26P/Grigg/Skjellerup (*17*).

High D excesses observed in interplanetary materials have long been attributed to interstellar chemistry, because large D enrichments (D/H > 0.01) are observed in the gas phase of cold molecular clouds (*7*). However, there is a strict upper limit on the fraction of crystalline relative to amorphous silicates in the interstellar medium (<0.2% by mass) (*18*). If the organic matter from the UCAMMs was a direct heritage of interstellar origin, one would expect the associated minerals to be dominated by amorphous silicates, which is not the case. Quite the opposite, the organic matter of the UCAMMs contains crystalline phases typical of silicates processed within the accretion disk (*19*), such as those observed both in anhydrous IDPs (*20*) and in the fine-grained fraction of Wild 2 particles (*21*). Therefore, the UCAMMs cannot be considered as a direct interstellar heritage but most probably sampled material (organic matter and minerals) from the protoplanetary disk itself.

Substantial D excesses have been identified at the molecular level in IOM from the Orgueil and Murchison meteorites, supporting an exchange mechanism between the organic matter and a local gaseous D-rich reservoir within the nascent solar system (*9*). Numerous astronomical observations demonstrate the occurrence of deuterated molecules in protoplanetary disks, some of them exhibiting large D/H variations (0.01 < D/H < 0.1) for radial distances between 30 and 70 AU (*22*). The large range of D/H ratios observed in the UCAMMs may be reminiscent of the D/H gradient that once existed at several tens of astronomical units from the young Sun.

Other than the bona fide Wild 2 particles returned by the Stardust mission, the assignment of a cometary or asteroidal origin to a given interplanetary dust particle remains speculative. The unmelted nature of the UCAMMs precludes high atmospheric entry velocities usually associated with a cometary origin. However, once released from their parent body, the trajectories of dust within that size range substantially evolve (as a result of resonances with giant planets, radiation pressure, the Poynting-Robertson effect, and solar wind drag), and cometary dust can

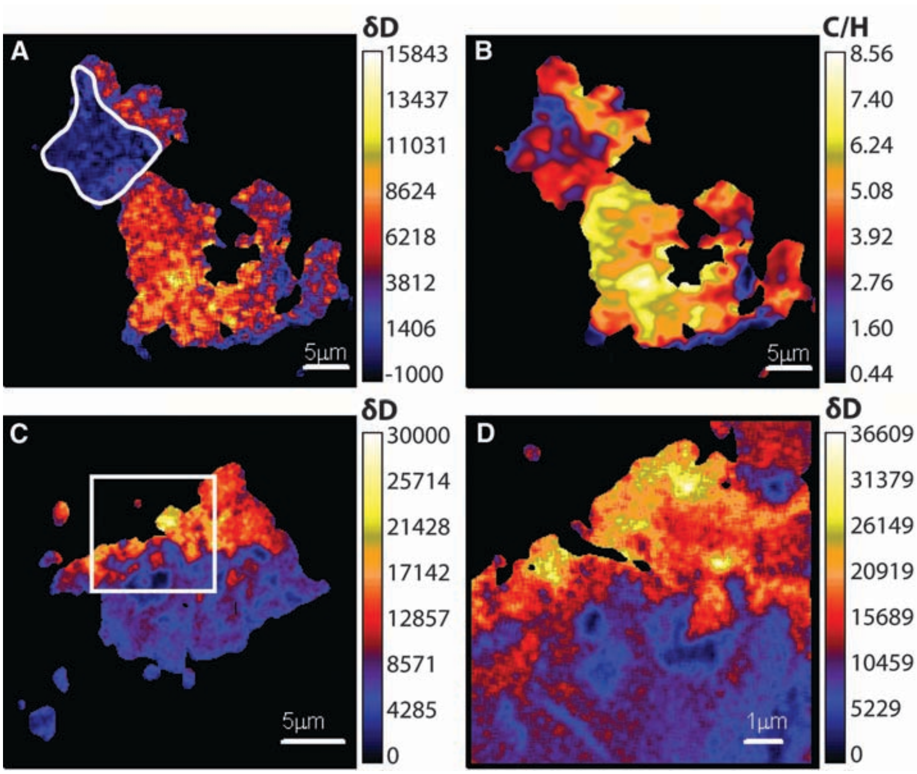

Fig. 3. NanoSIMS-50 (secondary ion mass spectrometry) isotopic and elemental maps of UCAMMs. (**A** and **B**) δD (‰) (*13*) (A) and C/H atomic ratio (B) of particle 19. The contour in (A) indicates a region with low D/H ratio (Fig. 4) (*13*). (**C**) δD (‰) map of particle 119. (**D**) Higher-magnification δD (‰) map of the zone indicated by the white rectangle in (C).

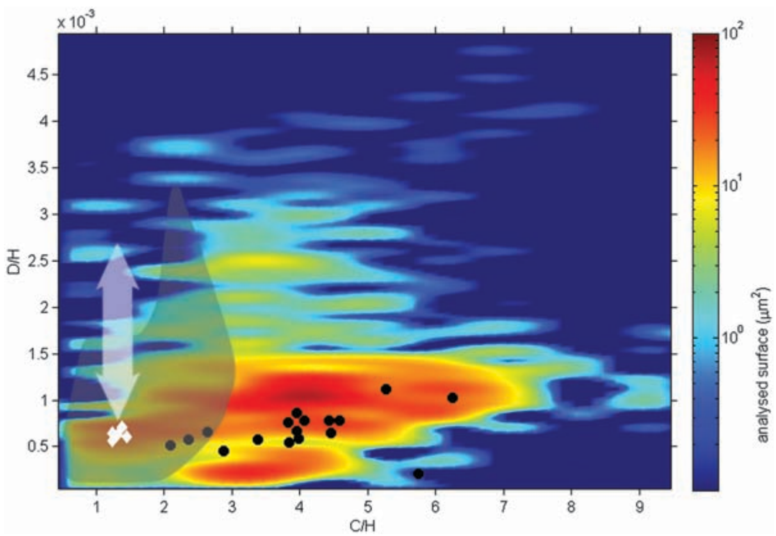

Fig. 4. Distribution of D/H versus C/H atomic ratios in particles 19 and 119 (*13*). The data from bulk IOM from CR (white diamonds), UOCs (black dots) (*10*), and the range of D-rich hot spots observed in primitive chondrites (*5*) (white arrow) and that from IDPs (*4*, *17*) (gray surface) are reported.

eventually have Earth-crossing orbits that are difficult to distinguish from typical asteroidal trajectories (*23*). Some chondritic porous anhydrous IDPs are believed to be of cometary origin, as assessed by their noble gas content, high porosity, high carbon content, and high D/H ratios (*3*, *24*, *25*). The exceptionally high carbon content of the UCAMMs equals or exceeds that of the most C-rich IDPs (*26*, *27*) and falls in the range of the CHON particles detected in comet 1P/Halley (*28*). Both the crystalline and amorphous silicates in the UCAMMs are comparable to those detected in the dust of different comets (*29*) and are compatible with the Wild 2 material (*30*). From these lines of evidence, we favor a cometary origin for these particles.

Both the large sizes and the high carbon content of the UCAMMs allow the direct in situ study of an early solar system organic compound together with its associated minerals, without any chemical extraction procedure. The association of extreme D-rich organic matter with high-temperature minerals confirms that material condensed or processed at close distances from the young Sun can be efficiently transported at several tens of astronomical units (*21*). The UCAMMs provide unique access to the intimate association of high- and low-temperature material from the protoplanetary disk in an unprecedented state of preservation.

References and Notes

1. R. Meier, T. C. Owen, *Space Sci. Rev.* **90**, 33 (1999).
2. K. D. McKeegan *et al.*, *Science* **314**, 1724 (2006).
3. S. Messenger, *Nature* **404**, 968 (2000).
4. J. Aléon, C. Engrand, F. Robert, M. Chaussidon, *Geochim. Cosmochim. Acta* **65**, 4399 (2001).
5. H. Busemann *et al.*, *Science* **312**, 727 (2006).
6. L. Remusat *et al.*, *Astrophys. J.* **698**, 2087 (2009).
7. T. J. Millar, A. Bennett, E. Herbst, *Astrophys. J.* **340**, 906 (1989).
8. Y. Aikawa, G. J. van Zadelhoff, E. F. van Dishoeck, E. Herbst, *Astron. Astrophys.* **386**, 622 (2002).
9. L. Remusat, F. Palhol, F. Robert, S. Derenne, C. France-Lanord, *Earth Planet. Sci. Lett.* **243**, 15 (2006).
10. C. M. O. D. Alexander, M. Fogel, H. Yabuta, G. D. Cody, *Geochim. Cosmochim. Acta* **71**, 4380 (2007).
11. I. Gilmour, in *Treatise on Geochemistry*, A. M. Davis, Ed. (Elsevier, Oxford, 2003), vol. 1, pp. 269–290.
12. M. Maurette *et al.*, *Nature* **351**, 44 (1991).
13. See supporting material on *Science* Online.
14. J. Duprat *et al.*, *Adv. Space Res.* **39**, 605 (2007).
15. T. Nakamura, T. Noguchi, Y. Ozono, T. Osawa, K. Nagao, *Meteorit. Planet. Sci.* **40** (suppl.), 5046 (2005).
16. S. Derenne, J. Rouzaud, C. Clinard, F. Robert, *Geochim. Cosmochim. Acta* **69**, 3911 (2005).
17. H. Busemann *et al.*, *Earth Planet. Sci. Lett.* **288**, 44 (2009).
18. F. Kemper, W. J. Vriend, A. G. G. M. Tielens, *Astrophys. J.* **609**, 826 (2004).
19. E. R. D. Scott, A. N. Krot, in *Chondrites and the Protoplanetary Disk*, A. N. Krot *et al.*, Eds. (Astronomical Society of the Pacific, San Francisco, 2005), pp. 15–53.
20. J. P. Bradley, *Geochim. Cosmochim. Acta* **58**, 2123 (1994).
21. D. Brownlee *et al.*, *Science* **314**, 1711 (2006).
22. C. Qi, D. J. Wilner, Y. Aikawa, G. A. Blake, M. R. Hogerheijde, *Astrophys. J.* **681**, 1396 (2008).
23. J. C. Liou, H. A. Zook, *Icarus* **123**, 491 (1996).
24. K. L. Thomas, L. P. Keller, G. E. Blanford, D. S. McKay, *Meteorit. Planet. Sci.* **27**, 296 (1992).
25. J. P. Bradley, in *Treatise on Geochemistry*, A. M. Davis, Ed. (Elsevier, Oxford, 2003), vol. 1, pp. 689–711.
26. K. L. Thomas, G. E. Blanford, L. P. Keller, W. Klöck, D. S. McKay, *Geochim. Cosmochim. Acta* **57**, 1551 (1993).
27. L. P. Keller *et al.*, *Geochim. Cosmochim. Acta* **68**, 2577 (2004).
28. M. E. Lawler, D. E. Brownlee, *Nature* **359**, 810 (1992).
29. D. H. Wooden, *Space Sci. Rev.* **138**, 75 (2008).
30. M. E. Zolensky *et al.*, *Science* **314**, 1735 (2006).

31. Supported by ANR grant 05-JC05-51407, FP6 Marie Curie Research Training Network "ORIGINS," ANR T-Tauri Chem, INSU (PNP), IN2P3, CNES, and CNRS. We are grateful to the French and Italian polar institutes, IPEV and PNRA, for their financial and logistic support. The NanoSIMS facility was established with funding from the CNRS, Région Île de France, MESR, and MNHN. The electron microscopy work in Lille is a national facility instrument INSU-CNRS. We are grateful to M. Maurette for stimulating exchanges and pioneering the micrometeorite research in Orsay; S. Derenne, E. Jacquet, E. Quirico, and G. Slodzian for enlightening discussions; and M. Horlok for careful reading of the manuscript.

Supporting Online Material

www.sciencemag.org/cgi/content/full/328/5979/PAGE/DC1
Materials and Methods
Figs. S1 to S4
Table S1
References

17 November 2009; accepted 24 March 2010
10.1126/science.1184832

Cross-Reacting Antibodies Enhance Dengue Virus Infection in Humans

Wanwisa Dejnirattisai,[1] Amonrat Jumnainsong,[1] Naruthai Onsirisakul,[1,2] Patricia Fitton,[1] Sirijitt Vasanawathana,[3] Wannee Limpitikul,[4] Chunya Puttikhunt,[5] Carolyn Edwards,[1] Thaneeya Duangchinda,[5] Sunpetchuda Supasa,[6] Kriangkrai Chawansuntati,[1] Prida Malasit,[5,6] Juthathip Mongkolsapaya,[1,6]*† Gavin Screaton[1]*†

Dengue virus co-circulates as four serotypes, and sequential infections with more than one serotype are common. One hypothesis for the increased severity seen in secondary infections is antibody-dependent enhancement (ADE) leading to increased replication in Fc receptor–bearing cells. In this study, we have generated a panel of human monoclonal antibodies to dengue virus. Antibodies to the structural precursor-membrane protein (prM) form a major component of the response. These antibodies are highly cross-reactive among the dengue virus serotypes and, even at high concentrations, do not neutralize infection but potently promote ADE. We propose that the partial cleavage of prM from the viral surface reduces the density of antigen available for viral neutralization, leaving dengue viruses susceptible to ADE by antibody to prM, a finding that has implications for future vaccine design.

Dengue virus (DENV) is a mosquito-borne virus infection found in tropical and subtropical areas of the world, with an estimated 50 to 100 million infections per year (*1*). A sequence variation of 30 to 35% allows DENV to be divided into four serotypes, and infection with one serotype does not provide protection from infection with the other serotypes, so that secondary or sequential infections are common (*2*, *3*). Serious complications of dengue haemorrhagic fever (DHF) are more likely during secondary versus primary infections (*2*, *3*).

In 1977, Halstead suggested antibody-dependent enhancement (ADE) to explain severe DENV infections (*4*). ADE has been widely studied and results from the high sequence divergence between DENV so that antibody to the first infection may not be of sufficient avidity to neutralize a secondary infection (*5*). The partial cross-reactivity may cause a degree of opsonization that promotes virus uptake into Fc-bearing cells such as monocytes and macrophages—a major site of DENV replication in vivo—leading to increased virus replication.

DENV envelope contains 180 copies of the E glycoprotein, which can be found in either dimeric or trimeric conformation (*6*). The structural precursor-membrane protein (prM) is a 166-amino-acid protein intimately associated in a 1:1 fashion with domain II of E (*7*) and is believed to act as a chaperone for the folding of E and to prevent the premature fusion of virus to membranes inside the producing cell. prM contains a furin cleavage site and is cleaved into a C-terminal M portion containing a transmembrane domain that remains associated with the virus particle, and an N-terminal 91-amino-acid precursor fragment that dissociates upon release of the virus from the infected cell.

B cells from seven DENV-infected individuals (table S1) were used to produce human mAb by using the method of Traggiai (*8*). Culture supernatants were screened against structural antigens by using whole virus and against nonstructural protein 1 (NS1) by means of enzyme-linked immunosorbent assay (ELISA).

Of 3020 cell lines, 301 screened positive, 73% reacted to the whole-virus ELISA for structural antigens, and 27% reacted to NS1. Positive super-

[1]Department of Medicine, Imperial College London, London W12 0NN, UK. [2]Faculty of Medical Technology, Mahidol University, Bangkok 10700, Thailand. [3]Pediatric Department, Khon Kaen Hospital, Khon Kaen 4000, Thailand. [4]Pediatric Department, Songkhla Hospital, Songkhla 90100, Thailand. [5]BIOTEC, NSTDA, Phatumthani 12120, Thailand. [6]Faculty of Medicine, Siriraj Hospital, Mahidol University, Bangkok 10700, Thailand.

*These authors contributed equally to this work.
†To whom correspondence should be addressed. E-mail: g.screaton@imperial.ac.uk (G.S.); j.mongkolsapaya@imperial.ac.uk (J.M.)